

PAPER • OPEN ACCESS

A Cutting-Edge Precision Agriculture Technology to Support the Sustainable Oil Palm Industry

To cite this article: H Santoso *et al* 2024 *IOP Conf. Ser.: Earth Environ. Sci.* **1308** 012053

View the [article online](#) for updates and enhancements.

You may also like

- [The effect of indigenous vegetations on the biological control of oil palm basal stem rot \(BSR\) disease caused by *Ganoderma* in peatlands](#)
Supriyanto, Purwanto, S H Poromarto et al.
- [Unmanned aerial vehicles \(UAV\) utilization for mapping the health of oil palm plants \(*Elaeis guineensis* Jacq.\)](#)
Charloq, A S Thoah, D Y Putra et al.
- [Discriminating the Severity of Basal Stem Rot Disease in Oil Palm \(*Elaeis guineensis* Jacq.\) Plantation Using Sentinel-2](#)
R D Handrian, B H Trisasongko and D R Panuju

PRIME
PACIFIC RIM MEETING
ON ELECTROCHEMICAL
AND SOLID STATE SCIENCE

HONOLULU, HI
Oct 6-11, 2024

Abstract submission deadline:
April 12, 2024

Learn more and submit!

Joint Meeting of
The Electrochemical Society
•
The Electrochemical Society of Japan
•
Korea Electrochemical Society

A Cutting-Edge Precision Agriculture Technology to Support the Sustainable Oil Palm Industry

H Santoso¹, M A Yusuf¹, S Rahutomo¹, Madiyanto¹ and Winarna¹

¹ Indonesian Oil Palm Research Institute

Corresponding author: hs_jmp@yahoo.com

Abstract. One of the most important factors in attaining sustainability in oil palm plantations is proper production input management in accordance with Good Agronomic Practices. For controlling plant disease and fertilizing, it can be started with an accurate monitoring technique to identify disease infection and the level of leaf nutrients in the field. The monitoring method should also be inexpensive, rapid, less time-consuming, and repeatable. This study has demonstrated how image classification (remote sensing) can be used to locate oil palm trees that have the Basal Stem Rot (BSR) disease and to estimate the nutritional level of the leaves. The healthy and BSR-infected palms had been effectively recognized and mapped using the remote sensing approach, which was used in conjunction with machine learning as well as a multispectral camera from a satellite and UAV. Furthermore, the use of a UAV and Mapir camera had resulted in a good prediction of N, P, K, and Mg content in the palm leaves; therefore, it may be practical to monitor leaf nutrient status in the oil palm plantations.

Keyword: Oil Palm, Basal Stem Rot, multispectral camera, UAV

1. Introduction

Sustainability has become a global issue in the oil palm industry. As a response to the issue, the Indonesian Ministry of Agriculture has issued Regulation No.11/Permentan/OT.140/3/2015 concerning ISPO (Indonesian Sustainable Palm Oil), which is mandatory for all oil palm plantations in Indonesia. The ISPO defines principles and criteria as guidance for planters to apply GAP (Good Agronomic Practices) so yield can be increased in an eco-friendly way. Two of the most critical agronomic practices in oil palm plantations are controlling plant disease and optimizing fertilizer input. For the plant disease, basal stem rot (BSR) caused by *Ganoderma boninense* is the most lethal disease of oil palm in Indonesia. Until now, no effective treatment for BSR has been reported; the treatments that have been undergone have only prolonged the life of the infected palm [1–4]. Thus, early detection of BSR is a vital strategy to control the disease [1]. Furthermore, fertilizers account for 40–50% of the total costs of field upkeep [5]. Similar to other crops, recommendations for fertilizer input in oil palm plantations are based on analyses of leaf nutrient contents [6,7], where the leaf samples are analyzed yearly in the lab [8,9].



In general, manual BSR-infected palm monitoring and laboratory leaf analysis are expensive, time-consuming, and laborious. Consequently, a rapid, quick, and low-cost alternative monitoring method for BSR and nutrient levels is needed. The remote sensing method offers many opportunities of potential for that purpose. The remote sensing technique is an example of precision agriculture (PA), where PA has been widely used to manage crop production inputs in an environmentally responsible manner [10]. This study demonstrates how remote sensing can be employed for predicting leaf nutrient level and identify early BSR infection in oil palm plantations.

2. Remote sensing techniques to identify BSR disease

2.1. Satellite imagery and machine learning

The data samples of healthy and infected palms for the learning model were adopted from [11]. As a general rule, yellowish foliage, necrosis on older leaves, more than two spear leaves, frond fracture, decaying basal stem, and fungal fruiting bodies on the trunk are symptoms of BSR infection in palms in the field. This study used 144 data samples, consisting of 99 healthy palms and 45 infected palms. The variables were the mean pixel values from the four bands of QuickBird imagery. The data were randomized with stratified random sampling based on the number of each class in the sampling data and separated into training and testing data. We split the data according to Liaghat's ratio [12], with 75% of the data being utilized for training and 25% for testing. A total of 144 data points—109 for training and 35 for testing—were used, while the learning algorithms were the support vector machine (SVM), random forest (RF), and classification and regression tree (CART) models.

Table 1 displays each model's accuracy levels. In comparison to the CART (Overall Accuracy (OA) = 80%, kappa value = 0.57) and SVM models (OA = 77%, kappa value = 0.52), the RF classifier model exhibited a higher OA of 91% and a kappa value of 0.81. The accuracy of the current study was higher than that of our previous study [11], particularly when using the RF classifier model to map healthy and unhealthy palms. User's accuracy and Mapping accuracy on unhealthy palm is lower than the healthy one. It is caused by difference of commission value, unhealthy's commission value higher than healthy's. The distribution map of healthy and sick oil palms was then created using the RF classifier model. When the model was applied in R software utilizing 49,793 palms, the segmentation process classified 37,518 healthy palms and 12,275 unhealthy palms (Figures 1 and 2).

Table 1. Accuracy levels for the classification models CART (classification and regression tree), RF (random forest), and SVM (support vector machine).

Actual	SVM			RF			CART		
	Healthy	Unhealthy	All	Healthy	Unhealthy	All	Healthy	Unhealthy	All
Healthy	18	2	20	22	1	23	19	2	21
Unhealthy	6	9	15	2	10	12	5	9	14
All	24	11	35	24	11	35	24	11	35
Producer's accuracy (%)	75	82		92	91		79	82	
User's accuracy (%)	90	60		96	83		91	64	
Mapping Accuracy (%)	69	53		88	77		73	56	
Overall Accuracy (%)		77			91			80	
Observed Agreement		0.77			0.91			0.80	
Expected Agreement		0.53			0.56			0.54	
Kappa value		0.52			0.81			0.57	

2.2. Unmanned aerial vehicle and multispectral camera

The data acquisition was performed at the Aek Pancur Research Station of the Indonesian Oil Palm Research Institute on August 1, 2019. The oil palm trees at the research station were first planted in 2002. A multispectral camera and an unmanned aerial vehicle (UAV) were used to capture images during the data acquisition process. Leaf samples were also collected, and healthy and BSR-infected oil palms were identified to provide ground truth data. We used the Mapir Survey 3 camera as a multispectral camera with three bands, namely red (660 nm), green (550 nm), and near-infrared/NIR (850nm). The Mapir camera was attached to the platform UAV T-tail Voltron model with a hand launch for take-off. The automatic record was set along the flight pathway, with 80% overlap between the flight pathway and 75% overlap within the flight pathway. The flight lasted 38 minutes, covered a distance of about 29.71 km, and had a flying altitude of 200 m. Before and after the flight mission, we took pictures of the calibration reflectance target (CRT). The CRT image was used for reflectance conversion by Mapir camera control (MCC) (<https://www.mapir.camera/pages/calibrating-images-in-mapir-camera-control-application>).

After identifying and observing 158 oil palm trees in the field, we found that 106 trees were healthy and 52 trees were infected by BSR. The symptoms of BSR-infected palms are the appearance of more than two unopened spear leaves, necrosis on the older leaves, fractured fronds, and fungal fruiting bodies on the oil palm trunk [13–16]. The mean pixel values of each oil palm canopy were extracted, while the random forest (RF) of machine learning was applied to classify healthy and infected oil palm trees by BSR disease, referring to our previous study [17] using three variables (red, green, and NIR). The model was built from 75% of the data as training data, and the remaining 25% were used as testing data to measure classification accuracy. The classification accuracy by the confusion matrix and kappa served as the goodness-of-fit parameters [17,18]. The classification model was applied to all oil palm trees in the 37.2 ha coverage area to produce the distribution map of healthy and BSR-infected oil palm.

Table 2. Results of the RF (*random forest*) classifier models with the Mapir images as a variable in terms of accuracy.

Model Actual	RF		
	Healthy	Unhealthy	All
Healthy	25	1	26
Unhealthy	7	6	13
All	32	7	39
PA (%)	78.13	85.71	
UA (%)	96.15	46.15	
Mapping accuracy (%)	75.76	42.86	
OA (%)		79.49	
Kappa		0.48	

Remarks: PA=producer accuracy; UA= user accuracy; OA= overall accuracy

The study's site, which has been confirmed to be an endemic area for BSR disease, has a flat landscape. Due to the data collecting time of 3:58–4:36 pm local time, the mosaic image (Figure 2) comprises portions with cloud shadow (darker view) and without cloud shadow (lighter view). The reflectance of oil palms had been impacted by the cloud shadow, as observed by the Mapir sensor and identified by the RF model. The accuracy and kappa value for the results of classification using the RF model were 79,49% and 0.48 (Table 2), respectively; the results could be classified as “middle”. The RF model was applied to 3,442 oil palms on 37.2 ha of land and revealed that 2,294 (66.65%) palms are healthy and 1,148 (33.35%) palms are infected by BSR (Figure 3).



Figure 1. Sample map showing the distribution of both healthy and unhealthy oil palm trees at Sites 1 and 2, respectively.

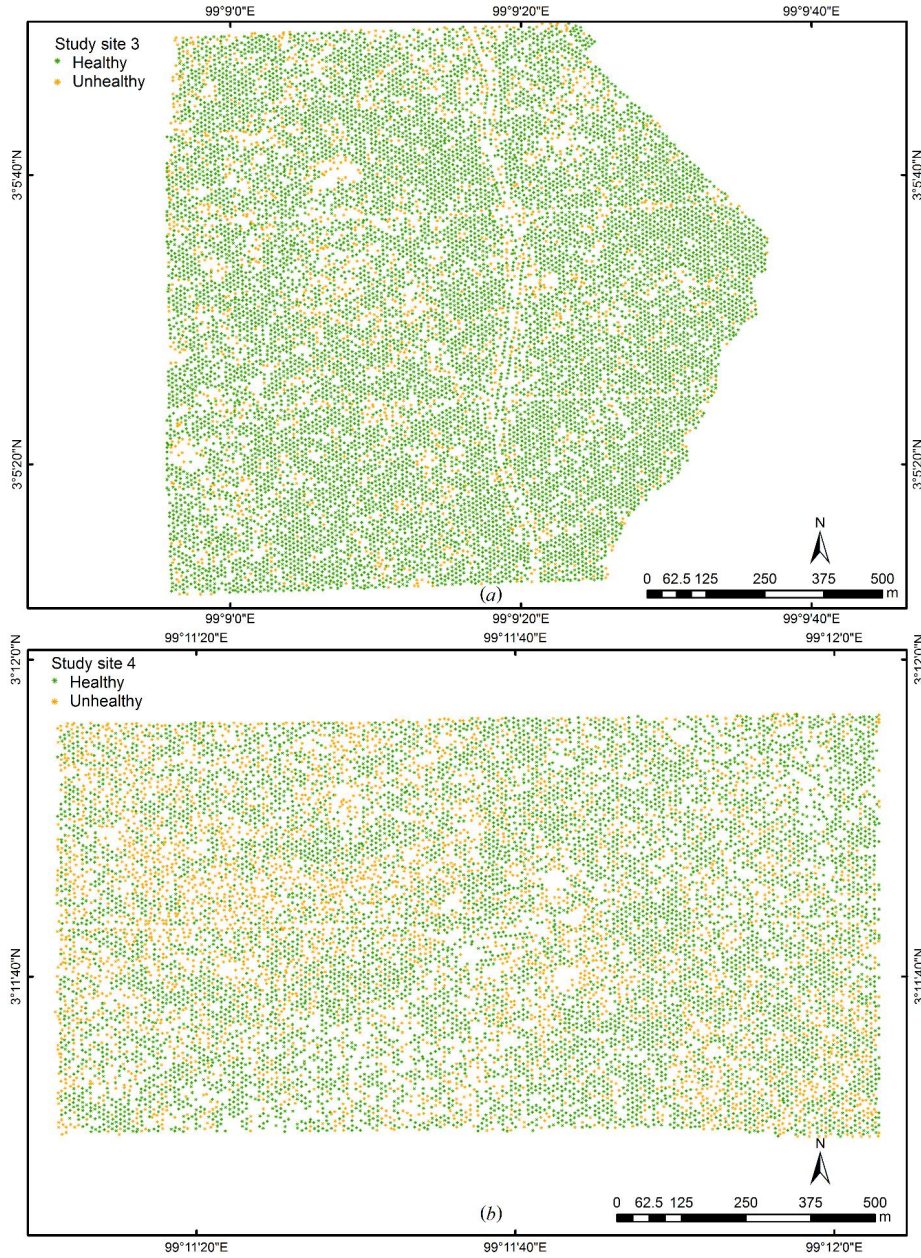


Figure 2. Sample map showing the distribution of both healthy and unhealthy oil palm trees at Sites 3 and 4, respectively.

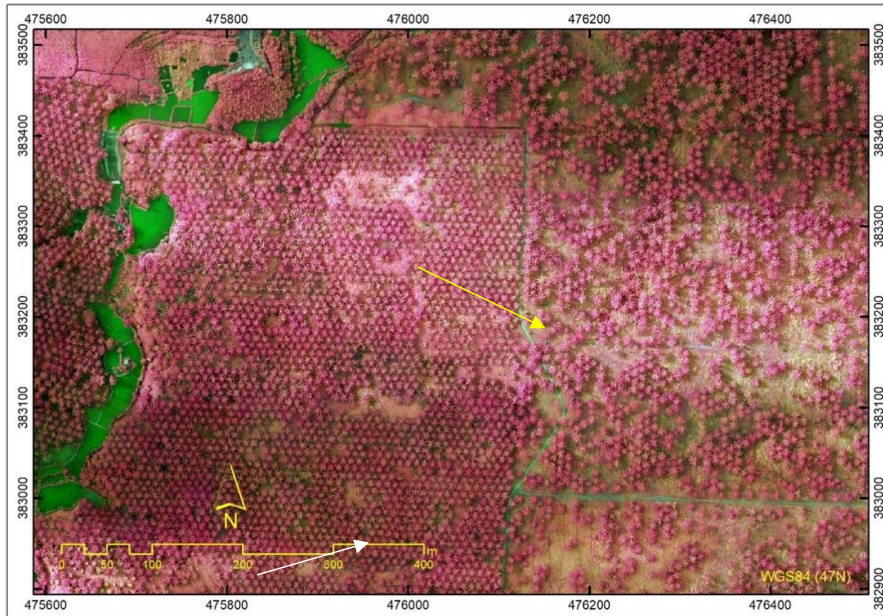


Figure 3. The mosaic image of the Mapir camera contains a part with cloud shadow (white arrow) and a part without cloud shadow (yellow arrow).

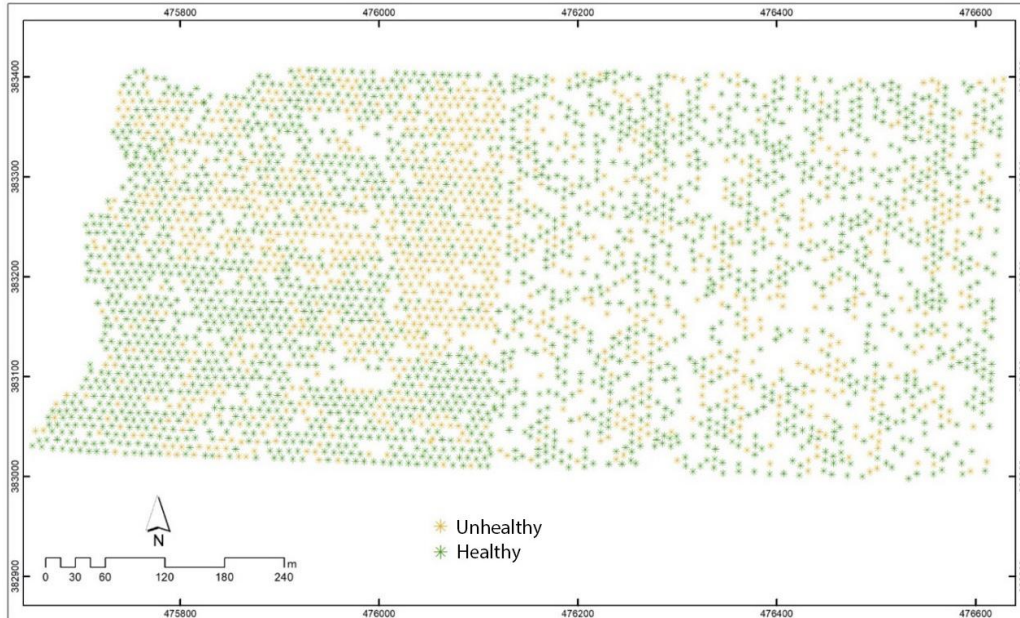


Figure 4. The distribution map of healthy and unhealthy (*basal stem rot* (BSR)-infected) oil palm trees using Mapir imagery

3. Remote sensing techniques for predicting leaf nutrients content

We collected twenty leaf samples from twenty oil palm trees for leaf nutrient contents (N,P,K,Ca, Mg, and B) analysis at IOPRI's lab. The methods for nutrient content analysis were Kjeldahl for N, atomic absorption spectrometry (AAS) for K, Ca, and Mg, and spectrometry for P and B [19,20] [19,20]. Three bands, namely normalized difference vegetation index (NDVI), green NDVI (GNDVI), and simple ratio (SR), were used as variables to predict leaf nutrient content. We used multivariate and multivariate polynomial regression to estimate N, P, K, Ca, Mg, and B content in the leaves. The *recursive feature elimination* (RFE) [21] was applied for variable selection in multivariate and multivariate polynomial regression with the random forest (RF) function (rfFuncs) in the Caret Package of R Studio software [22,23]. The adjusted R^2 and R^2 between the reference values and predicted values from the model's output of nutrient content prediction were the goodness-of-fit parameters.

Figures 4 and 5 display the characteristics of leaf nutrient content and predictor variables. The dominant categories for the level of leaf nutrient content were low for N and B, high for P and K, and normal for Mg. Furthermore, the distribution of leaf Ca content levels included low, normal, and high values. Table 3 shows the variables from the selection made using RFE and the RF function. Four of the variables were chosen to predict the leaf contents of N, P, and B, while six were chosen to predict the contents of K, Ca, and Mg.

Table 3. The variables selected from the RFE (*recursive feature elimination*) and RF (*random forest*) functions

Leaf nutrient	Variable						Variable count
	band1	band2	band3	NDVI	GNDVI	SR	
N	✓			✓	✓	✓	4
P	✓		✓	✓		✓	4
K	✓	✓	✓	✓	✓	✓	6
Mg	✓	✓	✓	✓	✓	✓	6
Ca	✓	✓	✓	✓	✓	✓	6
B	✓	✓		✓	✓		4

Table 4 displays the performance of multivariate and polynomial prediction models of leaf nutrient content. The multivariate prediction model was only suitable to predict K and Mg with high relationships ($R^2= 0,6577$ and Adj. $R^2= 0,4996$) and low relationships ($R^2= 0,3612$ and Adj. $R^2= 0,0664$), respectively. Meanwhile, the multivariate polynomial prediction model was suitable to predict N (polynomial degree 5 with $R^2= 0,9985$ and Adj. $R^2= 0,9713$), P (polynomial degree 4 with $R^2= 0,9415$ and Adj. $R^2= 0,7223$), K (polynomial degree 3 with $R^2= 0,9991$ and Adj. $R^2= 0,9837$), and Mg (polynomial degree 3 with $R^2= 0,993$ and Adj. $R^2= 0,8677$), but it was not suitable to predict Ca and B. Multivariate polynomial regression can be used to enhance the performance of linear regression [24] when there is an unclear relationship between the predictor and the dependent variable [25]. The leaf nutrient prediction using the best models in Table 4 that applied to all oil palm trees in the study area is shown in Figures 6 and 7.

Table 4. The performance of multivariate regression and multivariate polynomial regression of the prediction model of leaf nutrients content of N, P, K, Ca, Mg, and B from RFE (*recursive feature elimination*) of the RF (*random forest*) function

Leaf nutrient	Multivariate		Polynomial degree 2		Polynomial degree 3		Polynomial degree 4		Polynomial degree 5	
	R ²	Adj-R ²	R ²	Adj-R ²	R ²	Adj-R ²	R ²	Adj-R ²	R ²	Adj-R ²
N	0,0924	-0,1496	0,5983	0,3062	0,8131	0,4928	0,9079	0,5625	0,9985	0,9713
P	0,1896	-0,0265	0,6222	0,3474	0,8603	0,6207	0,9415	0,7223	0,9673	0,3795
K	0,6577	0,4996	0,8580	0,6146	0,9991	0,9837	-	-	-	-
Mg	0,3612	0,0664	0,8349	0,5520	0,9930	0,8677	-	-	-	-
Ca	0,1839	-0,1927	0,2899	-0,9273	0,9093	-0,7232	-	-	-	-
B	0,0854	-0,1585	0,1263	-0,5092	0,2691	-0,9838	0,4816	-2,2830	-	-

The NDVI and SR were always selected from RFE with the RF function to predict N, K, and Mg of leaf nutrient content. One of the vegetation indices frequently employed in remote sensing studies for estimating and monitoring green biomass plants as well as measuring leaf chlorophyll, particularly in high-density region, is the simple ratio (SR) equation [26]. The NDVI is very sensitive to green leaves in the low-density part, leaf area index (LAI), and canopy photosynthesis, while it is significantly affected by leaf shadow, cloud, and atmospheric conditions [26,27].

4. Conclusions

This study has demonstrated cutting-edge precision agriculture technology in controlling plant disease and managing leaf nutrients in oil palm plantations. The distribution of oil palm affected with BSR disease in oil palm plantations has potentially been identified and mapped using a remote sensing technology coupled with a multispectral camera from a satellite and UAV as well as machine learning. The UAV and Mapi camera have potentially been utilized to estimate the N, P, K, and Mg content of the leaves and to monitor the nutritional status of the leaves after fertilizing. By generating data from the field quickly and precisely, crop production inputs can be managed in an environmentally friendly way, which is fundamental to sustainability in oil palm plantations.

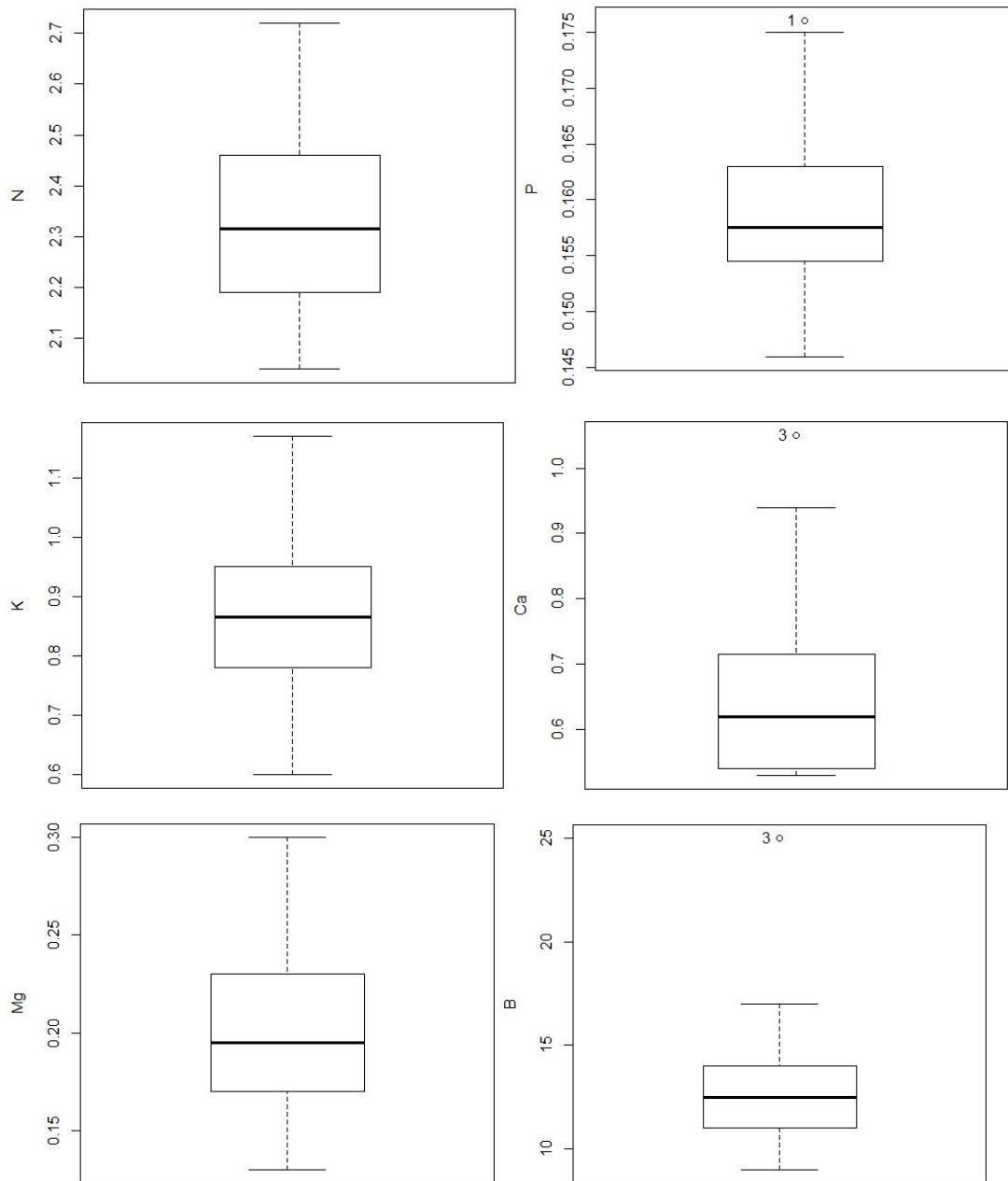


Figure 5. The boxplot showing the leaf's N, P, K, Ca, Mg, and B content.

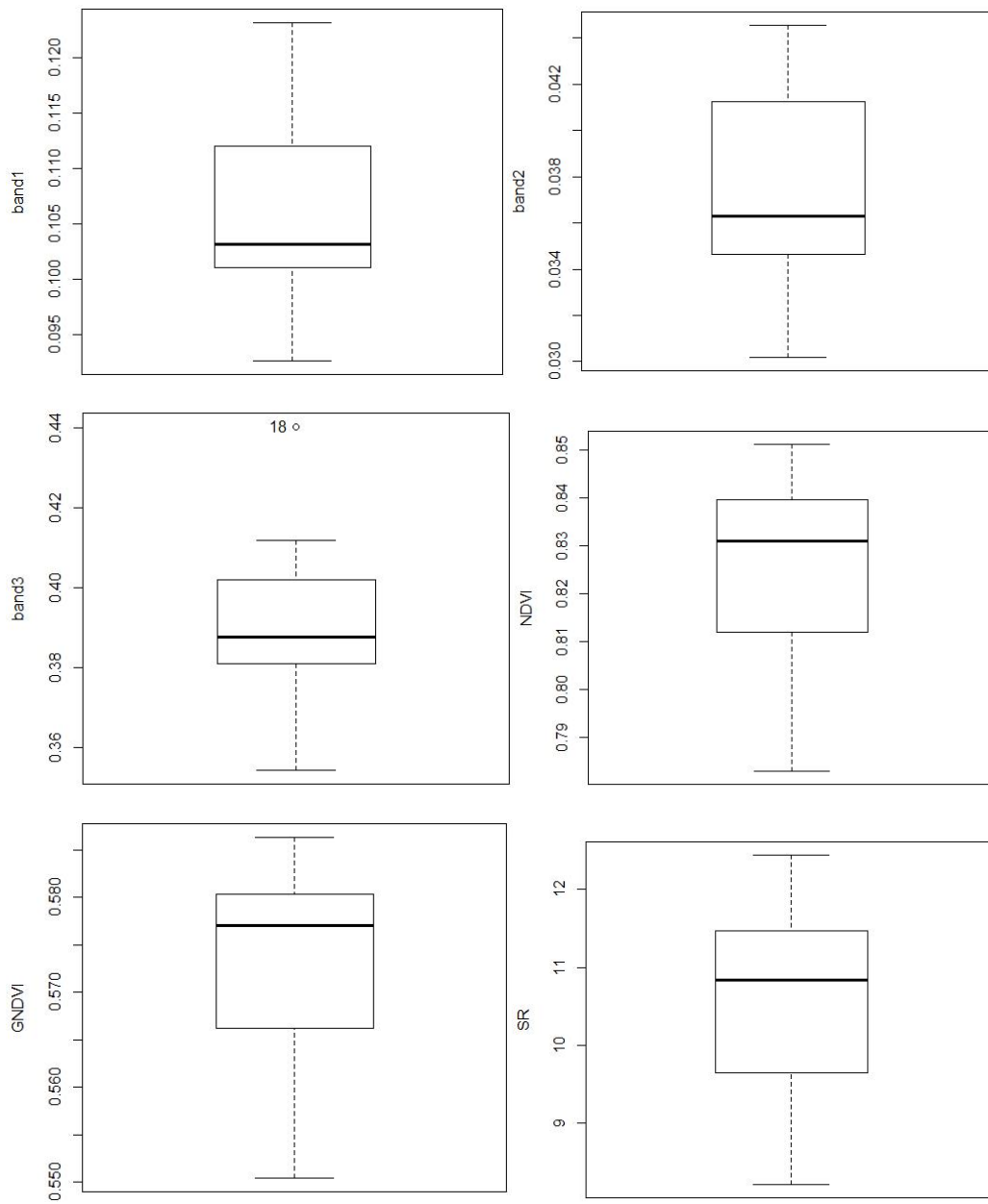


Figure 6. The boxplot showing the predictor variables (normalized difference vegetation index (NDVI), green NDVI (GNDVI), simple ratio (SR), band 1, band 2, and band 3)

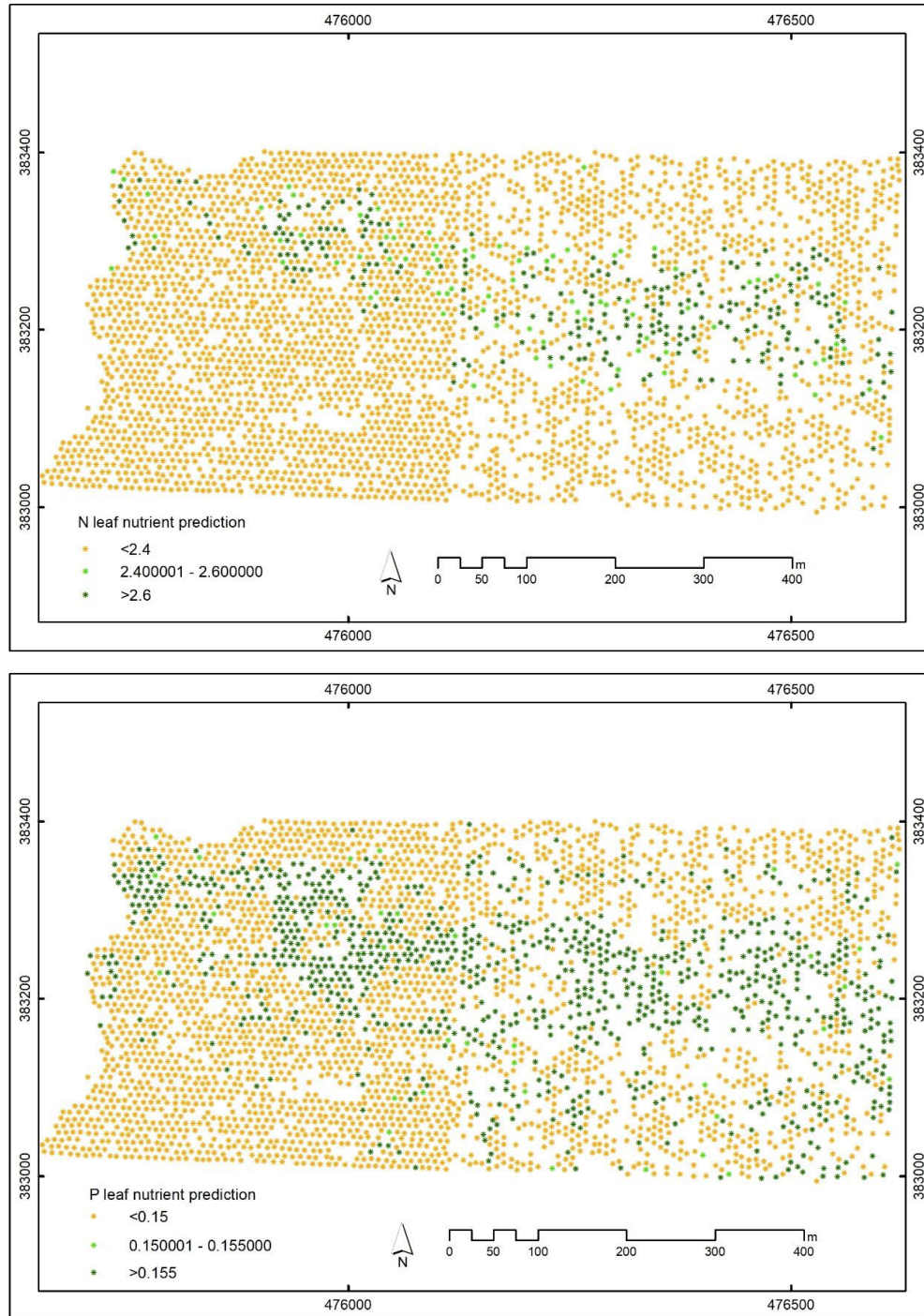


Figure 7. Sample map illustrating the predicted contents of N and P in the leaves for each oil palm tree in the study site.

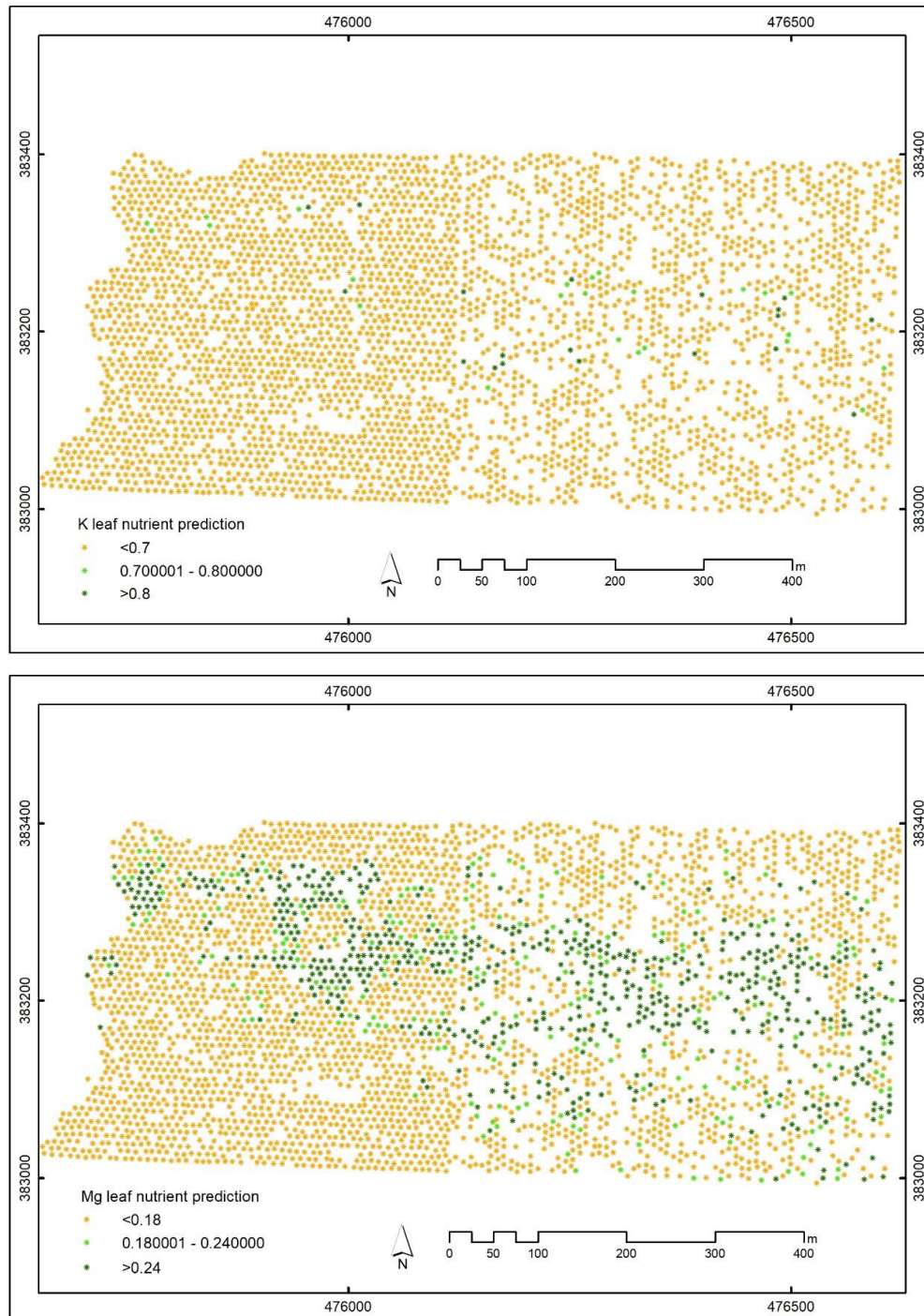


Figure 8. Sample map illustrating the predicted contents of K and Mg in the leaves for each oil palm tree in the study site.

5. References

- [1] Hushiarian R, Yusof N A and Dutse S W 2013 *Springerplus* **2** 555
- [2] Susanto A, Prasetyo A E, Priwiratama H, Wening S and Surianto S 2013 *J. Fitopatol. Indones.* **9** 123–6
- [3] Priwiratama H, Prasetyo A E and Susanto A 2014 *J. Fitopatol. Indones.* **10** 1–7
- [4] Priwiratama H and Susanto A 2014 *J. Agric. Sci. Technol.* **4** 103–11
- [5] Ng S 2002 *Crop Prod. Int. Symp. Role Potassium India. Potash Res. Inst. India, Int. Potash Institute, New Delhi.* 415–29
- [6] Pritts M and Heidenreich C 2012 Leaf and Soil Analysis Special Edition *New York Berry News. Cornell Univ. Coll. Agric. Life Sci.* **11**
- [7] Memon N, Memon K S and Hassan Z 2005 *Int. J. Agric. Biol.* **7** 824–31
- [8] Chapman G W and Gray H M 1949 *Ann. Bot.* **13** 415–433
- [9] Fairhurst T and Mutert E 1999 *Better Crop. Int.* **13**, No 1 48–51
- [10] Bongiovanni R and Lowenberg-Deboer J 2004 *Precis. Agric.* **5** 359–87
- [11] Santoso H, Gunawan T, Jatmiko R H, Darmosarkoro W and Minasny B 2011 *Precis. Agric.* **12**
- [12] Liaghat S, Ehsani R, Mansor S, Shafri H Z M, Meon S, Sankaran S and Azam S H M N 2014 *Int. J. Remote Sens.* **35** 3427–39
- [13] Ng S K 1972 *The Oil Palm, its Culture, Manuring and Utilisation* (Switzerland: International Potash Institute)
- [14] Corley R H V., J.J. H and B.J. W 1976 (Amsterdam: Elsevier Scientific Publ.)
- [15] Turner P D 1981 (Oxford: Oxford University Press)
- [16] Corley R H V and Tinker P B 2003 (Malden, MA: Blackwell Science Ltd.)
- [17] Santoso H, Tani H and Wang X 2017 *Int. J. Remote Sens.* **38** 4683–99
- [18] Santoso H, Tani H, Wang X, Prasetyo A E and Sonobe R 2019 *Int. J. Remote Sens.* **40** 1–23
- [19] Santoso H, Tani H, Wang X and Segah H 2019 *Int. J. Remote Sens.* **40** 1–22
- [20] Sulaeman, Suparto and Eviati 2005 *Analisis Kimia Tanah, Tanaman, Air, Dan Pupuk* ed F Agus (Bogor: Indonesian Soil Research Institute)
- [21] Gromski P S, Xu Y, Correa E, Ellis D I, Turner M L and Goodacre R 2014 *Anal. Chim. Acta* **829** 1–8
- [22] RStudio 2015 Integrated development environment (IDE) for R Code
- [23] Kuhn M 2015 *Compr. R Arch. Netw.*
- [24] Wei J, Chen T, Liu G and Yang J 2016 *Sci. Rep.* **6** 1–13
- [25] Priyanka Sinha 2013 *Int. J. Sci. Eng. Res.* **4** 962–5
- [26] Xue J and Su B 2017 *J. Sensors* **2017**
- [27] Kalaitzidis, C; Heinzl, V; Zianis D 2010 *Imagin[e,g] Eur. Proc. 29th Symp. Eur. Assoc. Remote Sens. Lab. Chania, Greece* 8